RSC Advances

ROYAL SOCIETY OF CHEMISTRY

www.rsc.org/advances

Synthesis, structures, and properties of seven transition metal coordination polymers based on a long semirigid dicarboxylic acid ligand

Yingying Bing, Meihui Yu, Ming Hu*

(Inner Mongolia Key Laboratory of Chemistry and Physics of Rare Earth Materials, School of Chemistry and Chemical Engineering, Inner Mongolia University, Hohhot 010021, China)

Abstract

Seven transition metal coordination polymers associated with a long dicarboxylic acid ligand have been synthesized under hydrothermal conditions, namely, $[ZnL(H_2O)]_n$ (**1**), $[CdL(H_2O)_2]_n$ (**2**), $[CoL(H_2O)_2]_n$ (**3**), $[MnL(phen)(H_2O)]_n$ (**4**), $\{[NiL(phen)]\cdot H_2O\}_n$ (**5**), $[CuL(bpp)_{0.5}]_n$ (**6a, 6b**), (H_2L = 1,4-Bis(4-oxy-1-benzene carboxylic acid)benzene, phen = 1,10-phenanthroline, bpp = 1,2-di(4-pyridyl)ethane). Compounds **1-6** have been characterized by the elemental analysis, IR spectra, TGA, powder X-ray diffraction (PXRD) and the single crystal X-ray crystallography. Compound **1** displays an undulating 2D layered structure. Isostructural **2** and **3** exhibit the three-dimensional framework structures containing the 1D channel. Compounds **4** and **5** show the similar 1D wavelike chain structures. Compounds **6a** and **6b** are two four-fold interpenetrated three-dimensional supramolecular isomers, and it is a remarkable fact that the semirigity of H_2L ligand has brought about the diverse structures of **6a** and **6b**. The solid state luminescence of **1** and **2** and magnetic properties of **3** were further investigated, respectively.

Introduction

Design and construction of metal–organic frameworks (MOFs) in the recent past decade have been attracted considerable interest not only because of their variety of intriguing architectures and topologies, but also owing to their potential applications in the aspects of gas storage and separation, fluorescent, magnetism, molecular recognition, catalysis and so on.[1-5] So far, the synthesis of MOFs with unique structures and properties is still a challenge for chemists because many factors may affect the self-assembly of MOFs, such as reaction solvent, pH value, temperature, metal-to-ligand ratio, etc.[6-8] Besides, the configurations of ligands, such as the length, rigidity and flexibility, symmetry and coordination sites must be considered, which play the critical roles in constructing MOFs.[9]

The rigid and semirigid multicarboxylic acid ligands are still good candidates for building MOFs on account of their rich coordination modes and various conformations.[10, 11] In the process of building MOFs, the semirigid aromatic multicarboxylate ligands can relatively easily regulate its configurations to enhance the structural diversity, in contrasting to the rigid ligands with difficult conformational changes.[12, 13] In addition, an effective and controllable route is to introduce auxiliary multidentate N-donor ligands. However, fewer studies about both the long semirigid carboxylate ligands and auxiliary multidentate N-donor ligands have been reported.[14–18] Also, supramolecular isomerism is one of the less common cases among MOFs. [19]

In this work, We selected 1,4-Bis(4-oxy-1-benzene carboxylic acid)benzene (H_2L) as the ligand

with the following reasons: (1) owning two carboxylate groups in symmetrical positions which can bond metal ions in different modes to produce diverse structures; (2) possessing two semirigid -O- spatial linkers permitting the benzene rings rotate which benefit for structural tunability; (3) to the best of our knowledge, MOFs based on such a long and semirigid H_2L have never been reported. As we expected, seven transition metal coordination polymers with diverse structures of a 2D layer, two isostructural 3D frameworks, two 1D wavelike chain and two isomers have been synthesized based on H_2L ligand. Meanwhile, the structures, thermal stabilities, luminescence and magnetic properties of some complexes were explored in detail.

Experimental section

Materials and general methods

The H_2L was synthesized according to the literature procedure.[20] All other reagents were used as received from commercial sources without further purification. Elemental analyses (C, H and N) were determined on Perkin-Elmer 2400 analyzer. The IR spectra were recorded as KBr pellets on a Nicolet Avatar-360 spectrometer in the 400-4000 cm^{-1} region. Thermogravimetric analysis (TGA) was performed on a Perkin-Elmer TG-7 analyzer heated from 25 to 800℃ under nitrogen atmosphere. Powder X-ray diffraction (PXRD) was performed on a PAnalytical Empyrean instrument by using Cu Kα radiation at room temperature. The luminescence spectra were measured on a FLS920 spectrophotometer.

Synthesis of complexes 1-6

$[ZnL(H_2O)]_n$ (1). A mixture of $Zn(NO_3)_2·6H_2O$ (0.1 mmol, 29.7 mg) and H_2L (0.1 mmol, 35.0 mg) in 10 mL of mixed H_2O-CH_3CN (5:5,v/v) was stirred for 30 min at room temperature and then was sealed in a 23 mL Teflon-lined stainless steel vessel, heated at 160°C for 72 h, kept 20 h at 100°C and followed by slow cooling to the room temperature at a rate of 2°C /h. The colorless crystalline product of **1** was obtained, isolated by filtration, then washed with H_2O and air-dried. Yield: 52% (based on Zn). Elemental analysis (%): Calcd for: $C_{20}H_{14}ZnO_7$, C 55.59, H 3.24; Found: C 55.61, H 3.27%. IR (KBr pellet): 1682.37(s), 1588.06(m)，1500.83(w)，1433.47(m)，1301.15(s), 1188.39(m)，943.92(m)，721.81(s).

$[CdL(H_2O)_2]_n$ (2). Complex **2** was synthesized by the same procedure used for preparing **1** except that $Cd(NO_3)_2·4H_2O$ (0.1 mmol, 30.8 mg), instead of $Zn(NO_3)·6H_2O$, was used as the starting material. After being cooled to room temperature, colorless crystal of **2** was collected, washed with H_2O, and air-dried. Yield: 57% (based on Cd). Elemental analysis (%): Calcd for: $C_{20}H_{16}CdO_8$, C 48.32, H 3.22%; Found: C 48.29, H 3.21%. IR (KBr pellet): 1597.08(s)，1535.68(m)，1482.88(s)，1405.44(s)，1301.15(s)，1220.78(s)，1100.04(w)，785.28(m).

$[CoL(H_2O)_2]_n$ (3). A mixture of $Co(NO_3)_2·6H_2O$ (0.1 mmol, 29.2 mg) and H_2L (0.05 mmol，17.7 mg) was dissolved in 0.02 mol/L NaOH solution (10 mL). The final mixture was placed in a 23 mL Teflon-lined stainless steel vessel and heated at 140°C for 72 h, and then followed by slow cooling to the room temperature at a rate of 2°C/ h. The purple crystal of **3** was collected, washed with H_2O, and air-dried. Yield: 49% (based on Co). Elemental analysis (%): Calcd for: $C_{20}H_{16}CoO_8$, C 54.14, H 3.61%; Found: C 54.15, H 3.63%. IR(KBr pellet): 1637.52(s), 1497.66(m), 1424.25(m), 1399.80(m), 1284.32(w), 1243.44(s), 1163.78(w), 1104.30(w), 876.59(w), 785.23(m), 698.89(w), 618.21(w).

$[MnL(phen)(H_2O)]_n$ (4). A mixture of $MnCl_2·4H_2O$ (0.1 mmol, 19.8 mg), H_2L (0.05 mmol，17.3 mg), phen (0.1 mmol, 20.1 mg) and H_2O (12 mL) was stirred for 30 min at room temperature

and was sealed in a 23 mL Teflon-lined stainless steel vessel, heated at 160°C for 72 h and followed by slow cooling to the room temperature at a rate of 2 °C /h. The light yellow crystalline product of **4** was obtained, isolated by filtration, then washed with H_2O and air-dried. Yield: 58% (based on Mn). Elemental analysis (%): Calcd for: $C_{32}H_{22}MnN_2O_7$, C 63.84, H 2.66, N, 4.66%; Found: C 63.87, H 2.67, N 4.64%. IR (KBr pellet): 3398.22(s), 1684.95(s), 1606.11(s),1538.44(m), 1485.05 (s), 1415.55(s), 1305.97(m), 1245.36 (m), 1164.05(m), 1099.42(m), 1011.45(w), 885.06(m), 790.92(m), 692.21 (m), 649.47(w).

{[NiL(phen)]·H_2O}$_n$ (5). A mixture of $NiCl_2·6H_2O$ (0.05 mmol, 11.9 mg), H_2L (0.05 mmol, 17.5 mg), phen (0.05 mmol, 9.9 mg) was dissolved in 0.02 mol/L NaOH solution (10 mL) and was sealed in a 23 mL Teflon-lined stainless steel vessel, heated at 160°C for 72 h and followed by slow cooling to the room temperature at a rate of 2 °C/h. The green crystalline product of **5** was obtained, isolated by filtration, then washed with H_2O and air-dried. Yield: 63% (based on Ni). Elemental analysis (%): Calcd for: $C_{16}H_{11}NNi_{0.5}O_{3.5}$, C 63.45, H 3.64, N 4.63%; Found: C 63.47, H 3.67, N 4.64%. IR (KBr pellet): 3403.41(s), 1675.25(m), 1611.88(s), 1525.56(s), 1418.12(s), 1298.28(w), 1222.73(s), 1169.33(s), 1103.10(s), 875.73(m), 781.92 (m), 724.20 (m), 640.87 (m).

[CuL(bpp)$_{0.5}$]$_n$ (6a). A mixture of $Cu(NO_3)_2·3H_2O$ (0.05 mmol, 12.1 mg), H_2L (0.05 mmol, 17.5 mg), bpp (0.1 mmol, 18.1 mg) was dissolved in 10mL of mixed H_2O-CH_3CN (5:5,v/v) and was sealed in a 23 mL Teflon-lined stainless steel vessel, heated at 160°C for 72 h, kept 72 h at 100°C and followed by slow cooling to the room temperature at a rate of 2°C /h. The green crystalline product of **6a** was obtained, isolated by filtration, then washed with H_2O and air-dried. Yield: 68% (based on Cu). Elemental analysis (%): Calcd for: $C_{26}H_{17}CuNO_6$, C 62.03, H 3.38, N 2.78%; Found: C 62.07, H 3.36, N 2.71%. IR (KBr pellet): 3389.36(s), 1704.25(m), 1603.57(m), 1549.70(w), 1403.22(s), 1361.75(m), 1316.12(m), 1226.05 (m), 1163.68(m), 1014.05(w), 952.86(w), 874.85(m), 748.90 (w), 657.55 (m).

[CuL(bpp)$_{0.5}$]$_n$ (6b). Complex **6b** was obtained by the same procedure used for preparing **6a** except that $CuCl_2·2H_2O$ (0.05 mmol, 8.5 mg), instead of $Cu(NO_3)_2·3H_2O$, was used as the starting material. After being cooled to room temperature, green crystal of **6b** was collected, washed with H_2O, and air-dried. Yield: 67% (based on Cu). Elemental analysis (%): Calcd for: $C_{26}H_{17}CuNO_6$, C 62.04, H 3.38, N 2.78 %; Found: C 62.09, H 3.31, N 2.81%. IR (KBr pellet): 1647.47(m)，1613.39(m), 1585.04(m)，1519.07(s), 1443.88(s)，1326.50 (s)，1204.43(s)，1174.98(m)，1147.61(w)，1024.11(w), 887.10(m), 786.77(m), 671.13(w).

X-ray crystallography

Crystallographic data for the compounds were collected on a Bruker Apex Smart CCD diffractometer with graphite-monochromated Mo-Kα radiation (λ = 0.71073) using the ω-scan technique at room temperature. All the structures were solved by direct methods with SHELXS-97 and refined with the full-matrix least-squares $|F|^2$ technique using the SHELXL-97 program.[21] The position of non-hydrogen atoms were refined with anisotropic displacement parameters. The hydrogen atoms were set in calculated positions and refined as riding atoms with a common isotropic thermal parameter. The crystallographic data for the seven crystals are listed in Table 1. The selected bond lengths and angles of them are listed in Table S1.

Table 1. The crystallographic data for **1–6**

Compound	**1**	**2**	**3**	**4**	**5**	**6a**	**6b**
Formula	$C_{20}H_{14}ZnO$	$C_{20}H_{16}CdO_8$	$C_{20}H_{16}CoO_8$	$C_{32}H_{22}MnN_2O_7$	$C_{16}H11NNi_{0.5}O_{3.5}$	$C_{26}H_{17}CuNO_6$	$C_{26}H_{17}CuNO_6$
Formula	431.7	496.74	443.26	601.46	302.61	502.95	502.96
T/K	293(2)	293(2)	293(2)	296(2)	293(2)	293(2)	293(2)
Crystal	monoclinic	orthorhombic	orthorhombic	monoclinic	Orthorhombic	Triclinic	Monoclinic
Space group	$P\,2_1/c$	*Pnma*	*Pnma*	$P2_1$	*Pccn*	*P*-1	*C*2/*m*
a(Å)	36.745(3)	5.7913(3)	5.6453(13)	6.3847(12)	5.83670(16)	10.6053(8)	14.434(2)
b(Å)	5.5792(8)	40.564(2)	40.200(9)	21.746(4)	22.1190(6)	11.1058(13)	19.805(4)
c(Å)	8.6871(8)	7.9028(4)	7.6789(19)	10.1336(19)	20.4593(5)	12.1321(17)	10.6271(13)
α(°)	90	90	90	90	90	114.559(13)	90
b(°)	92.931(8)	90	90	105.085(4)	90	111.070(10)	130.336(9)
γ(°)	90	90	90	90	90	96.515(8)	90
V(Å3)	1778.6(3)	1856.51(16)	1742.7(7)	1358.5(4)	2641.33(12)	1153.1(2)	2315.7(6)
Z	4	4	4	2	8	2	4
*D*calc(g	1.612	1.777	1.689	1.47	1.522	1.449	1.443
μ(mm−1)	1.423	1.224	1.035	0.54	1.533	1.702	1.695
F(000)	980	992	908	618	1248	514	1028
*R*int	0.0664	0.0137	0.0497	0.0353	0.0329	0.0451	0.0666
GOOF	1.111	1.07	1.067	1.086	1.032	1.014	1.008
*R*1*a*	0.1105	0.0326	0.0380	0.0509	0.0386	0.0500	0.0844
*ωR*2*b* [I >	0.3164	0.1243	0.0813	0.1385	0.1057	0.1089	0.1984
*R*1(all data)	0.1305	0.0361	0.059	0.0594	0.0444	0.0741	0.1532
*wR*2(all data)	0.3485	0.1329	0.0868	0.1445	0.1115	0.1237	0.2529

[a] $R_1 = \Sigma||F_o| - |F_c||/\Sigma|F_o|$. [b] $\omega R_2 = [\Sigma[\omega(F_o^2-F_c^2)^2]/\Sigma\omega(F_o^2)^2]^{1/2}$

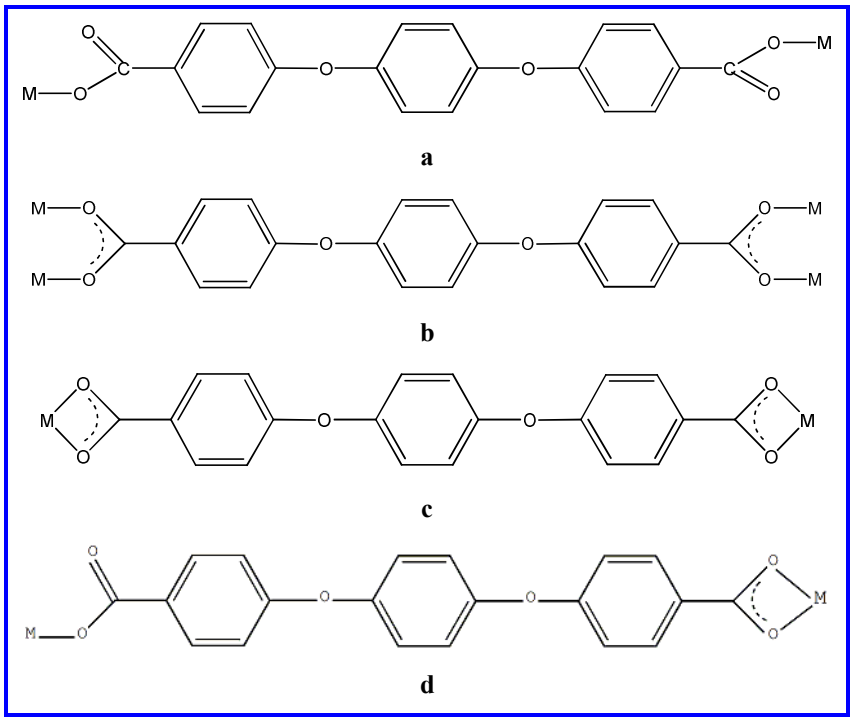

Scheme 1. Coordination modes of H_2L

Results and discussion

Structural description of 1

Single-crystal X-ray structure determination reveals that compound **1** crystallizes in the monoclinic *P* $2_1/c$ space group and exhibits a two-dimensional framework. The asymmetric unit of **1** contains one Zn(II) ion, one L^{2-} ligand, and one coordinate water molecule. Here, each Zn(II) center adopts a distorted tetrahedron geometry with the ZnO_4 coordination environment by three carboxylate oxygen atoms from L^{2-} ligand, and one from water molecule (Fig. 1a). The Zn-O bond lengths range from 1.943(11) to 1.987(8) Å, which is similar to the reported.[22] The L^{2-} connects Zn(II) ions in two different modes: bis(monodentate) and bis(bridging bidentate) (Scheme 1a, 1b). It is noteworthy that L^{2-} linker holds two Zn(II) ions in two different distances of 19.158 and 18.102 Å, respectively. In addition, L^{2-} ligand in bis(monodentate) mode connects two Zn(II) to form a parallelogram (19.16× 4.42 $Å^2$), while the other in bis(bridging bidentate) mode links two Zn(II) to form a different parallelogram (18.10 × 4.42 $Å^2$), sharing an edge with the former (Fig. S1). Note that the two coordination patterns of L^{2-} ligands are arranged alternatively to display an undulating layered structure in **1** (Fig. 1b)

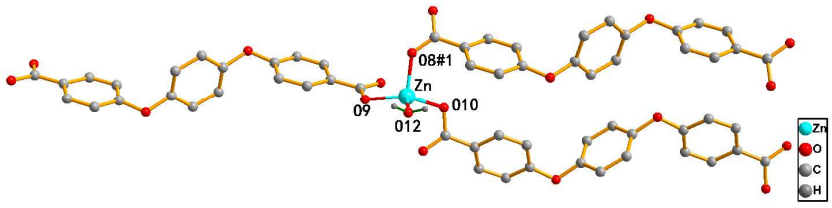

(a)

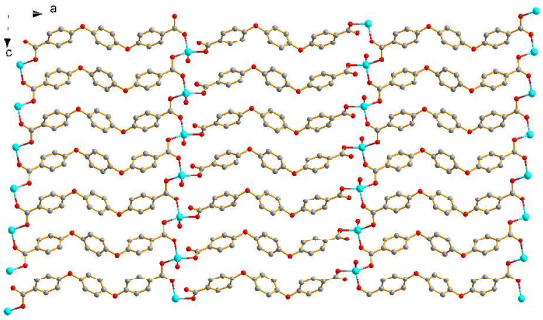

(b)

Fig.1 (a) Coordinated environment of Zn (II) ion; (b) The 2D sheet architecture of **1**.

Structural description of 2 and 3

The structural investigation reveals that compounds **2** and **3** are isostructural and crystallize in the orthorhombic *Pnma* space group, the structure of **2** is described in detail as the representative example. The asymmetric unit of **2** is comprised of one Cd(II) ion, one L^{2-} ligand, one μ_2-H_2O molecule, and one terminal water molecule. The hepta-coordination environment of Cd(II) ion is fulfilled by four carboxylate oxygens from two L^{2-} ligands through bis(chelating bidentate) mode (Scheme 1c) and three from coordinated water molecules to generate a distorted pentagonal bipyramid geometry (Fig. 2a). The M-O bond lengths are in the range of 2.254(5)-2.418(3) Å with Cd(II) and 2.072(3)−2.2846(18) Å with Co(II) ions, respectively, which are similar to those observed in the reported complexes.[23] Each L^{2-} ligand bridges with the metal centers and extends along the *c* axis to form the 1D chain, and adjacent 1D chains are pillared by a μ_2-H_2O from perpendicular direction to furnish a 2D layer in the *ac* plane (Fig. 2b). Further, neighboring layers are interconnected through another μ_2-H_2O linkers to generate the 3D framework (Fig. 2c).

It is interesting to note that there exist rectangular grids in the *ab* plan with a size of 40.56 × 4.12 $Å^2$ in complex **2** and 40.20 × 3.95 $Å^2$ in **3**, which are built by four L^{2-} ligands and four metal ions (Fig. S2). The rectangular grids are further extended by μ_2-H_2O linkers to form a 1D channel along the *b* axis.

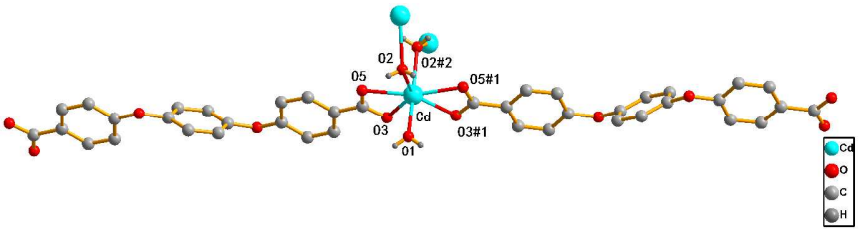

(a)

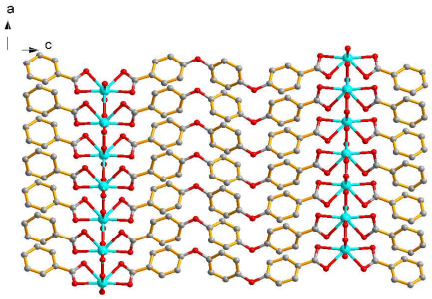

(b)

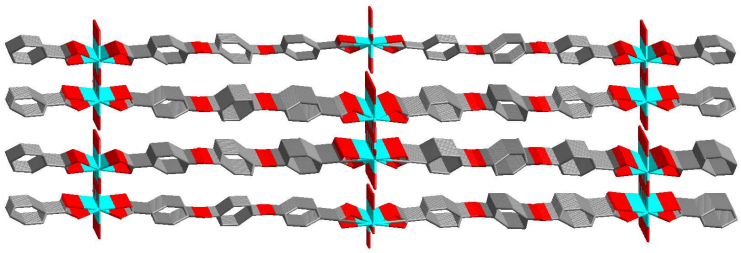

(c)

Fig.2 (a) Coordinated environment of Cd (II) ion; (b) A view of the 2D sheet of **2** along the *b* axis; (c) The 3D architecture of **2**

Structural description of 4

Complex **4** crystallizes in the monoclinic system with space group $P2_1$. There are one Mn(II) ion, one L^{2-} ligand, a coordinated water molecule and a phen molecule in the asymmetric unit of **4**. The coordination environment and atom connectivity for **4** are shown in Fig. 3a. Mn(II) ion is six-coordinated with a distorted octahedron geometry, which is coordinated by three carboxylate O atoms from two different L^{2-} ligands, one O atom coming from terminal water molecule and two nitrogen atoms from phen. The Mn-O bond distances range from 2.109(4) to 2.426(4) Å; the Mn–N bond lengths are from 2.246(4) to 2.302(4) Å, which are well-matched to those observed in the reported complexes.[24] Each L^{2-} ligand link neighboring Mn(II) ions in monodentate and chelating bidentate mode (Scheme 1d) to lead to a 1D wave-like chain along *a* axis (Fig. 3b). There are existing hydrogen bonds including intramolecular and intermolecular interactions, which are formed between water molecules and carboxylate oxygen atoms. The chains connected each other to generate a 2D layer along the *c* axis on account of the interactions of hydrogen bonds. (Fig. 3c). At the same time, there exist π-π interactions between the two benzene rings from two adjacent layers with a center-to-center distance of about 3.7Å. Finally, the 1D chains are combined through the intermolecular hydrogen bonds and the π-π interactions to exhibit a 3D supramolecular architecture (Fig. 3d).

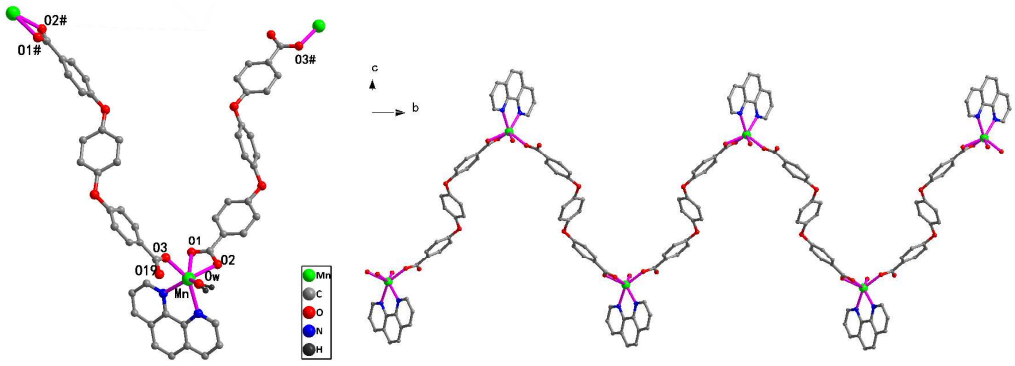

(a) (b)

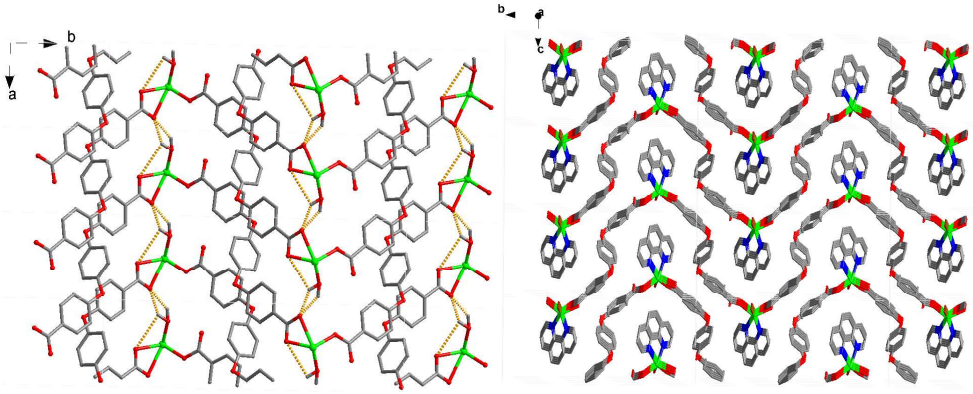

(c) (d)

Fig.3 (a) Coordinated environment of Mn(II) ion; (b) A view of 1D chain along *b* axis; (c) The 2D sheet formed by hydrogen bonds along *c* axis (phen was omitted); (d) The 3D supramolecular architecture of **4**

Structural description of 5

Complex **5** crystallizes in the orthorhombic space group *Pccn*. Its asymmetric unit consists of a crystallographically independent Ni(II) ion, a deprotonated L^{2-} ligand, a phen and a lattice water molecule. Each Ni(II) ion is coordinated by four carboxylate oxygen atoms from two L^{2-} ligands in bis(chelating bidentate) mode (Scheme 1c) and two nitrogen atoms from phen, which forms distorted octahedral coordination mode (Fig. 4a). The Ni-N bond distances are 2.0415(16) Å, and the Ni-O bond distances range from 2.0483(15) to 2.1638(13) Å. These are similar to values found in other complexes.[25] Comparing with **4**, complex **5** has the similar 1D wave-like chain structure but differ in coordination modes of L^{2-} ligand (Fig. 4b). In the meantime, the chains extended by hydrogen bonds formed between free water and carboxylate groups to generate a 2D layer view along the *c* axis (Fig. 4c). In addition, the adjacent layers stack together to give the supramolecular 3D framework by the C-H···π interactions with the distance of 3.003−3.606 Å (Fig. 4d).

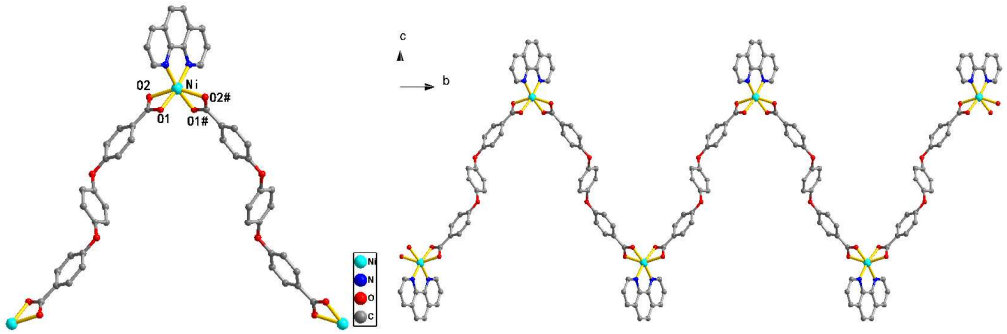

(a) (b)

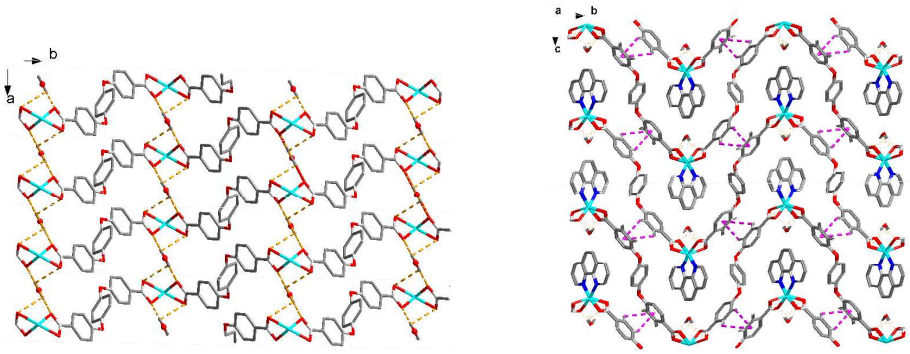

(c) (d)

Fig.4 (a) Coordinated environment of Ni(II) ion; (b) A view of 1D chain along the *b* axis; (c) The 2D sheet formed by hydrogen bonds along *c* axis (phen was omitted); (d) The 3D architecture of **5** formed by the C-H···π interactions (pink dotted lines, distance: 3.003−3.606 Å)**.**

Structural description of 6a

Complex **6a** crystallizes in the triclinic space group *P*-1. The asymmetric unit contains one Cu(II) ion, one deprotonated L^{2-} ligand and half a bpp. As shown in Fig. 5a, each Cu(II) is square-pyramidally coordinated by four carboxylate oxygen atoms from four L^{2-} ligands at the basal positions and one nitrogen atom from one bpp at the apical position. It is worthy to note that there are two kinds of L^{2-} ligands differing only in angular distortions, 118.5 (4)° around O3 atom and 117.8(4)° around O6 atom, respectively. The Cu−N bond distance is 2.180(3) Å, and the Cu−O bond distances are vary in the range of 1.957(3)−1.967(2) Å, which correspond to normal bond lengths found in other Cu complexes.[26] Two crystallographically equivalent Cu(II) cations are bridged by four carboxylate groups adopting bridging bidentate mode (Scheme 1b) to generate a distorted dinuclear Cu(II) "paddle-wheel" secondary building unit (SBU) with a Cu···Cu distance of 2.6424(8) Å. The paddle-wheel is bridged by L^{2-} ligands to form a 2D network with parallelogram grids, and the size is 19.56 ×19.57 $Å^2$ (Fig. 5b). There are also two parallelogram grids in complex **6a** with the sizes of 19.57 × 13.68 $Å^2$ (Fig. S3a) and 19.56 × 13.68 $Å^2$ (Fig. S3b), respectively, which are built by two kinds of L^{2-} ligands and bpp and Cu(II) cations. The layers of grids are further connected by bpp to form a 3D coordination polymer network (Fig. 5c). To simplify the structure of **6a**, the L^{2-} ligand can be regarded as a two-connected node, bpp can be viewed as a two-connected linker and the dinuclear centers as 6-connected nodes, so the whole network could be viewed as a 2-nodal (2,6)-connected net with the point symbol $\{4^{12}.6^3\}$, and the overall structure of **6a** is four-fold interpenetrated framework (Fig. 5d).

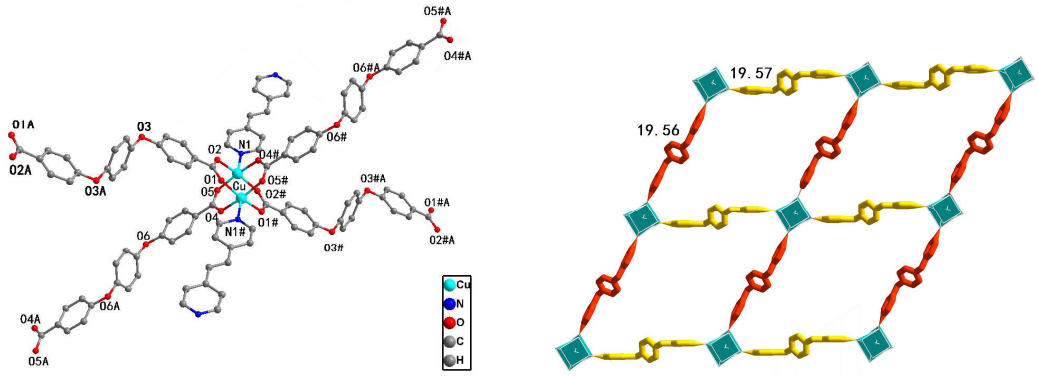

(a) (b)

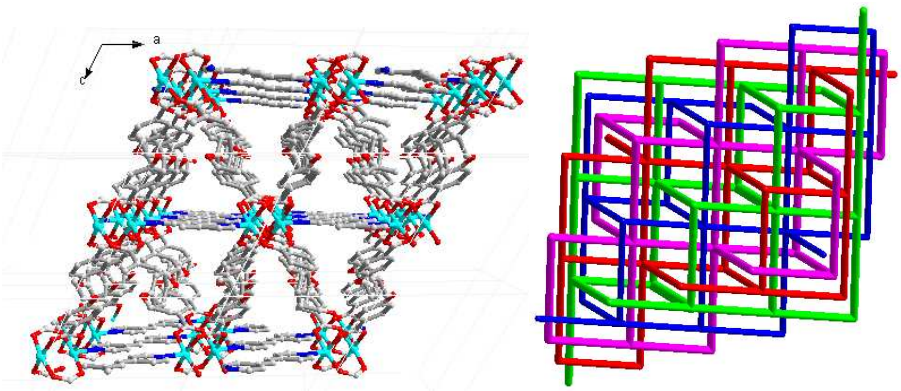

(c) (d)

Fig.5 (a) Coordinated environment of Cu(II) ion in **6a**; (b) The 2D network bridged by two kinds of L^{2-} ligands with a size of 19.56 ×19.57 $Å^2$; (c) The 3D network of 6a; (d) The four-fold interpenetrated framework of **6a**

Structural description of 6b

Compound **6b** crystallizes in the monoclinic space group *C*2/m. Complex **6a** and **6b** have the same chemical compositions with a small difference in the relative angular distortion of the L^{2-} ligands. Thus, **6a** and **6b** may be considered as examples of supramolecular isomerism owing to different torsion angles of L^{2-} ligands in **6a** and **6b**. Compound **6b** contains a similar "paddle -wheel" SBU as **6a**, but the difference is that the four O atoms at the basal plan are coming from the same kind of L^{2-} ligands with a torsion angle 118.6(7)° around O3 (Fig. 6a). The Cu−N bond distance is 2.167(8) Å, and the Cu−O bond distances are in the range of 1.950(5)−1.977(5) Å, which correspond to normal bond lengths found in other Cu complexes.[27] The paddle-wheel are bridged by L^{2-} ligands to form a 2D network with rhombic grids, and the size is 19.54 ×19.54$Å^2$ (Fig. S4a). There are also parallelogram grids in complex **6b** with a size of 19.54 × 13.68 $Å^2$ (Fig. S4b), which are built by L^{2-} ligands and bpp. The layers are further connected to form a 3D coordination polymer architecture (Fig. 6b). The whole framework can be viewed as a 2-nodal (2,6)-connected net with the point symbol of $\{4^{12}.6^3\}$, upon considering L^{2-} as 2-connected node and the dinuclear centers as 6-connected nodes. Finally, the framework of **6b** is four-fold interpenetrated framework (Fig. 6c).

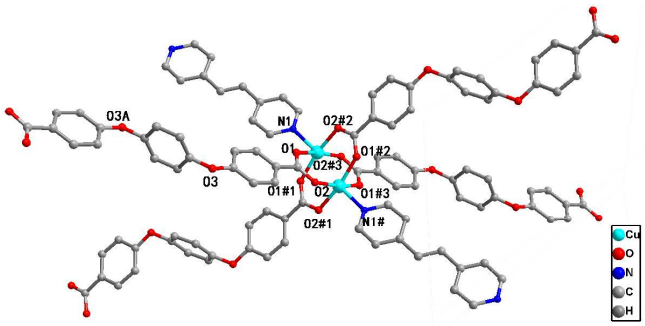

(a)

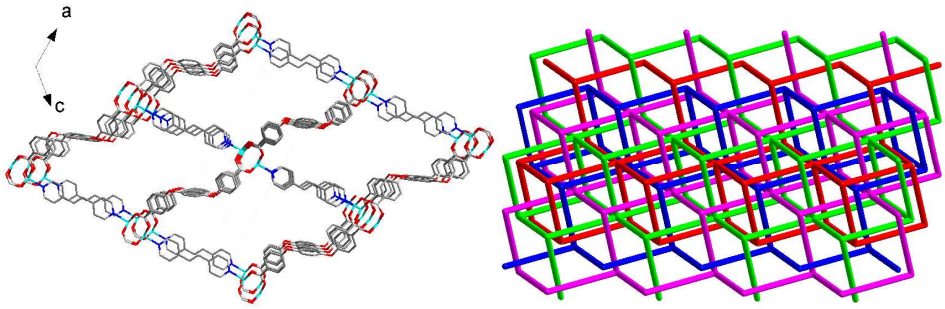

(b) (c)

Fig.6 (a) Coordinated environment of Cu(II) ion in **6b**; (b) the 3D network of **6b**; (c) The four-fold interpenetrated framework of **6b**

The structural differences of 6a and 6b.

As already indicated, both complex **6a** and **6b** contain the same molecular composition, that is, the paddle-wheel units are connected by four L^{2-} bridges and two bpp molecules to present the different 3D grid structures. In fact, the only difference between two structures is the torsional angles of H_2L: there are two angles of ether C-O-C in H_2L for 118.5 (4)° and 117.8 (4)° in **6a**, respectively; and it exist only a C-O-C torsional angle of 118.6 (7) ° in **6b**. It is worthy to note that the semirigity of H_2L ligand has brought about the diverse structures of **6a** and **6b**.

Photoluminescence properties

Generally, d^{10} complexes are promising to exhibit the photoluminescence properties. The solid-state photoluminescence of H_2L ligand and complexes **1** and **2** were investigated at room temperature, as shown in Fig. 7. The H_2L displays maximal emission peaks at 325 nm and 380 nm (λ_{ex} = 270 nm), which could probably be attributed to intraligand π*→π and π*→n transitions.[28] Compound **1** exhibits two emission bands centered at 540 and 610 nm (λ_{ex} = 297 nm), which are red-shifted 215 and 230 nm in comparing with that of H_2L and could be assigned to the ligand-to-metal charge transfer (LMCT).[29] Compound **2** shows the dual emission peaks at 350 nm and 420 nm (λ_{ex} =300nm), which is red-shifted 25 and 40 nm compared with that of H_2L and it is probably assigned to intraligand transitions.[30] The difference in luminescence spectra between **1** and **2** may probably be assigned to the different coordination environments of Zn(II) and Cd(II) ions. The luminescent properties of **1** and **2** can make them good candidates for the functional photoluminescent materials.

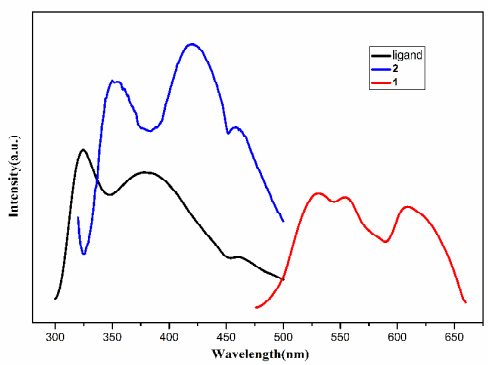

Fig.7 Photoluminescence spectra of **1**, **2** and H_2L ligand in the solid state at room temperature.

Magnetic property

The temperature dependent molar magnetic susceptibility of compound **3** was measured from 2

K to 300 K at an applied field of 1000 Oe. The data is shown in Fig. 8 as plots of $\chi_M T$ and χ_M^{-1} versus T. For **3**, the $\chi_M T$ value of 2.89 cm^3 K mol^{-1} at 300 K is higher than the expected spin-only value of Co(II) ion for S = 3/2 (1.875 cm^3 mol^{-1} K, g = 2.0), which could be attributed to the orbital contribution arising from Co(II) centre.[31] Upon cooling the sample, the $\chi_M T$ value decreases gradually, which indicates an antiferromagnetic interactions between Co(II) ions in compound **3**.[32] The inverse magnetic susceptibility curve shows a linear behavior in 50−300 K range and obeys the Curie−Weiss law, χ_M = C/(T−θ), with C = 2.99 cm3 K mol−1 and θ = −24.62 K. The negative θ value also suggests an antiferromagnetic coupling between Co(II) ions.[33]

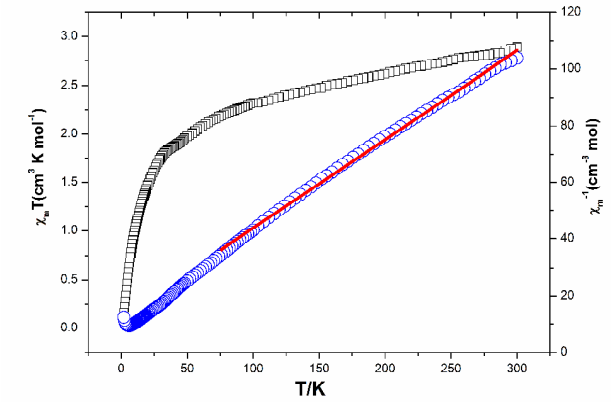

Fig.8 Temperature dependence of the χ_MT and χ_M^{-1} curve for complex **3**.The red line represents the fit to the Curie-Weiss law.

PXRD and Thermogravimetric analysis

The pure phases of complexes **1- 6** were confirmed by PXRD measurements, and the results are shown in Fig. S5. Meanwhile, each PXRD pattern of the as-synthesized sample is consistent with the simulated one.

The thermal stabilities of **1**−**6** were examined and the results are shown in Fig. S6. Complex **1** experiences a weight loss of 4.80% between ca. 120−150 °C, which corresponds to the liberation of coordinate water molecules (calcd 4.16%), and then decomposes step by step. The TGA curves of **2** and **3** are very similar for their similar structure. From 75 to 900 °C, there are several apparent weightlessness steps. A weight loss of approximately 7.19% between 85 and 140 °C for **2** (8.48% between 100 and 152 °C for **3**) is equivalent of losing of coordinate water molecules (calcd 7.24% for 2, 8.12% for 3). **4** and **5** undergo weight losses of 2.30% and 5.45%, respectively, which can be assigned to the losses of coordinated and free water molecules (calcd 2.99% for **4** and 5.95% for **5**), and the frameworks of **4** and **5** remain stable up to 300°C. For complex **6a** and **6b**, it does not contain guest molecules, the TG curve is almost flat until 305 °C, then appears a significant skeleton decomposition.

Conclusion

In summary, seven diverse transition coordination polymers of 1,4-Bis(4-oxy-1-benzene carboxylicacid)benzene have been prepared by the hydrothermal method. Complex **1** is an undulating 2D layer structure. Compounds **2** and **3** display the isomorphic 3D frameworks. Compounds **4** and **5** exhibit the similar supermolecular structures with undulated chains by introducing the auxiliary phen ligand. Compounds **6a** and **6b** are isomers which present different 3D structures containing diverse grids. The photoluminescent properties of **1** and **2** were investigated, which could be assigned to the ligand-to-metal charge transfer for **1** and intraligand

charge transition for **2**. The magnetic property of **3** was exploited, which reveals in the presence of an antiferromagnetic interactions between Co(II) ions.

Acknowledgements

This work is financially supported by the National Natural Science Foundation of China (No. 21361017), Inner Mongolia Natural Science Foundation of China (No. 2012MS0214) and the Scientific and Technological Key Research Project of Inner Mongolia Colleges & Universities (NJZZ12012).

References

1 (a) M. O'Keeffe, O. M. Yaghi, *Chem. Rev.* 2012, **112**, 675. (b) B. G. Rachel, S. B. Youn, E. W. Christopher, Q. S. Randall, *Chem. Rev.* 2012, **112**, 703.

2 (a) Y. J. Cui, Y. F. Yue, G. D. Qian, B. L. Chen. *Chem. Rev*. 2012, **112**, 1126. (b) J. Demel, P. Kubát, F. Millange, J. Marrot, I. Císařová, K. Lang. *Inorg. Chem*. 2013, **52**, 2779.

3 (a) G. L. Zhuang, L. Tan, W. L. Chen, J. Q. Bai, X. Zhong, J.G. Wang, *CrystEngComm*. 2014, **16**, 6963-6970

4 T. Ishiwata, Y. Furukawa, K. Sugikawa, K. Kokado, K. Sada, *J. Am. Chem. Soc*. 2013, **135**, 5427

5 (a) C. Janiak, *Dalton Trans*. 2003, 2781.(b) L. Q. Ma, C. Abney, W. B. Lin, *Chem. Soc. Rev.* 2009, **38**, 1248.

6 (a) F. P. Huang, H. D. Bian, Q. Yu, J. L. Tian, H. Liang, S. P. Yan, D. Z. Liao, P. Cheng . *CrystEngComm*. 2011, **13**, 6538. (b) M. Eddaoudi, J. Kim, N. Rosi, D. Vodak, J. Wachter, M. O'Keeffe, O. M. Yaghi, *Science*. 2002, **295**, 469.

7 (a)J. Liu, H. B. Zhang, Y. X. Tan, F. Wang, Y. Kang, J. Zhang, *Inorg. Chem*. 2014, **53**, 1500. (b) M. H. Yu, M. Hu, Z. T. Wu, H. Q. Su, Inorg. Chim. Acta. 2013, **408**, 84.

8 (a) H. Furukawa, J. Kim, N. W. Ockwig, M. O'Keeffe, O. M. Yaghi, *J. Am. Chem. Soc*. 2008, **130**, 11650. (b) X. Zhou, P. Liu, W. H. Huang, M. Kang, Y. Y. Wang, Q. Z. Shi, *CrystEngComm*. 2013, **15**, 8125. (c) Y. Zhang, W. W. Ju, X. Xu, Y. Lv, D. R. Zhu, Y. Xu, *CrystEngComm*. 2014, **16**, 5681. (d) P. Mahata, M. Prabu, S. Natarajan, *Inorg. Chem*. 2008, **47**, 8451.

9 (a) D. F. Sun, S. Q. Ma, Y. X. Ke, T. M. Petersen, H. C. Zhou, *Chem. Commun*. 2005, 2663. (b) D. S. Deng, L. L. Liu, B. M. Ji, G. J. Yin, C. X. Du, *Cryst. Growth Des.* 2012, **12**, 5338.

10 (a) X. L. Wang, C. Qin, E. B. Wang, Y. G. Li, Z. M. Su, *Chem. Commun.* 2005, **43**, 5450. (b) R. Q. Zou, R. Q. Zhong, M. Du, T. Kiyobayashi, Q. Xu, *Chem. Commun*. 2007, 2467.

11 (a) Q. Li, W. Zhang, O. S. Miljanic, C. B. Knobler, J. F. Stoddart, O. M. Yaghi, Chem. Commun. 2010, **46**, 380. (b) J. An, S. J. Geib, N. L. Rosi, *J. Am. Chem. Soc.* 2010, **132**, 38. (c) Q. Yue, Q. Sun, A. L. Cheng, E. Q. Gao, Cryst. Growth Des. 2010, **10**, 44. (d) A. Lan, K. Li, H. Wu, L. Kong, N. Nijem, D. H. Olson, T. J. Emge, Y. J. Chabal, D. C. Langreth, M. Hong, J. Li, *Inorg. Chem.* 2009, **48**, 7165. (e) C. Marchal, Y. Filinchuk, D. Imbert, J. C. G. Bunzli, M. Mazzanti, *Inorg. Chem.* 2007, **46**, 6242.

12 F. Dai, J. Dou, H. He, X. Zhao, D. Sun, *Inorg. Chem*. 2010, **49**, 4117.

13 (a) Z. Guo, R. Cao, X. Wang, H. Li, W. Yuan, G. Wang, H. Wu, J. Li, *J. Am. Chem. Soc*. 2009, **131**, 6894. (b) T. F. Liu, J. Lü, Z. Guo, D. M. Proserpio, R. Cao, *Cryst. Growth Des.* 2010, **10**, 1489. (c) T. F. Liu, J. Lu, X. Lin, R. Cao, *Chem. Commun*. 2010, **46**, 8439. (d) Z. J. Lin, T. F. Liu, B. Xu, L. W. Han, Y. B. Huang, R. Cao, *CrystEngComm*. 2011, **13**, 3321. (e)

T. F. Liu, J. A. Lu, C. B. Tian, M. N. Cao, Z. J. Lin, R. Cao, *Inorg. Chem.* 2011, **50**, 2264.

14 (a) Y. W. Lin, B. R. Jian, S. C. Huang, C. R. Huang, K. F. Hsu, *Inorg. Chem*. 2010, **49**, 2316. (b) P. Lama, A. Aijaz, S. Neogi, L. J. Barbour, P. K. Bharadwaj, *Cryst. Growth Des*. 2010, **10**, 3410.

15 W. T. Yang, M. Guo, F. Y. Yi, Z. M. Sun, *Cryst. Growth Des*. 2012, **12**, 5529.

16 (a) S. B. Ren, L. Zhou, J. Zhang, Y. L. Zhu, Y. Z. Li, H. B. Du, X. Z. You, *CrystEngComm.* 2010, **12**, 1635. (b) L. L. Liang, S. B. Ren, J. Zhang, Y. Z. Li, H. B. Du, X. Z. You, *Cryst. Growth Des.* 2010, **10**, 1307.

17 G. B. Li, J. M. Liu, Y. P. Cai, C. Y. Su, *Cryst. Growth Des.* 2011, **11**, 2763.

18 J. Yang, J. F. Ma, Y. Y. Liu, S. R. Batten, *CrystEngComm*. 2009, **11**, 151.

19 J. P. Zhang, X. C. Huang, X. M. Chen, *Chem. Soc. Rev*. 2009, **38**, 2385.

20 X. L. Zhang, Y. T. Li, J. Zhang, *Joumal of the Hebei Academy of Sciences*. 2007, **24**, 63.

21 (a) G.M. Sheldrick, Acta Crystallogr. 2008, **64**, 111-112. (b) G.M. Sheldrick, SHELXL-97, Program for Crystal Structures Refinement, University of Gottingen, Germany, 1997.

22 L. Luo, K. Chen, Q. Liu, Y. Lu, O. Taka-aki, G. C. Lv, Y. Zhao, W. Y. Sun, *Cryst. Growth Des.* 2013, **13**, 2312.

23 (a) H. A. Habib, A. Hoffmann, H. A. Hoppe, C. Janiak, *Dalton Trans*. 2009, 1742. (b) Q. Chu, Z. Su, J. Fan, O. Taka-aki, G. C. Lv, G. X. Liu, W. Y. Sun, U. Norikazu, *Cryst. Growth Des.* 2011, **11**, 3885.

24 D. F. Sun, S. Q. Ma, Y. X. Ke, *Chem. Commun*. 2005, 2663.

25 D. Sarma, K. V. Ramanujachary, S. E. Lofland, T. Magdaleno, S. Natarajan, *Inorg. Chem.* 2009, **48**, 11660.

26 L. Q. Ma, W. B. Lin, *J. Am. Chem. Soc*. 2008, **130**, 13834.

27 A. H. Robert, H. H. Zhao, X. Ouyang, G. Giulio, C. Jerry, R. D. Kim, *Inorg. Chem*. 1999, **38**, 144.

28 S. Q. Zhang, F. L. Jiang, M. Y. Wu, J. Ma, Y. Bu, M. C. Hong, *Cryst. Growth Des*. 2012, **12**, 1452.

29 S. L. Zheng, J. H. Yang, X. L. Yu, X. M. Chen, W. Wing-Tak, *Inorg. Chem*. 2004, **43**, 830

30 H. Y. He, H. D. Yin, D. Q. Wang, H. Q. Ma, G. Q. Zhang, D. F. Sun, *Eur. J. Inorg. Chem*. 2010, 4822

31 S. Bhattacharya, A. Goswami, B. Gole, S. Ganguly, S. Bala, S. Sengupta, S. Khanra, R. Mondal, *Cryst. Growth Des.* 2014, **14**, 2853.

32 T. Ma, M. X. Li, Z. X. Wang, J. C. Zhang, M. Shao, X. He, *Cryst. Growth Des*. 2014, **14**, 4155.

33 K. L. Cao,Y. P. Zhang, Y. N. Cai, X. W. Xu, Y. L. Feng, *J. Solid State Chem*. 2014, **215**, 34.